

Adaptive backstepping control of wheeled inverted pendulums models

Rongxin Cui · Ji Guo · Zhaoyong Mao

Received: 22 March 2014 / Accepted: 28 August 2014 / Published online: 12 September 2014
© Springer Science+Business Media Dordrecht 2014

Abstract In this paper, the state feedback control of wheeled inverted pendulum (WIP) used for mobile transportation has been investigated. The dynamic unstable balance and nonholonomic constraints inherent degrade the performance when the WIP operates in path-following mode. Through a suitable coordinates transformation, the WIP model is formulated into a parametric strict feedback form. Then, backstepping-based adaptive control is designed to achieve output tracking for the WIP. Simulation results are provided to show the effectiveness of the control proposed.

Keywords Backstepping · Adaptive control · Wheeled inverted pendulum · Path-following

1 Introduction

The control of wheeled inverted pendulum (WIP) has invoked a lot of research interests in recent years [1–12]. Typical applications of the WIP system include the baggage transportation and navigation [13]. In general, WIP has two torque inputs driving both wheels

and three degrees of freedom (DOF), including the forward and rotation of the platform, and the tilt angle of the pendulum, i.e., it follows an underactuated configuration. In addition, its dynamics is also nonlinear such that the WIP becomes an underactuated nonlinear system [1, 2, 5, 14–16]. Various control methods have been proposed for the nonholonomic/underactuated systems in past years [8, 17–20, 26]. A neural network-based nonlinear control for a nonholonomic mobile robot was proposed in [8]. A passivity-based control using interconnection and damping assignment was proposed for underactuated mechanical systems in [19]. A nonlinear control was designed for the mechanical system with an unactuated cyclic variable in [20]. For the high-order nonholonomic systems which described in the power chained form, a discontinuous feedback-based control was proposed in [21]. A bidirectional approach-based path planning was presented for a class of nonholonomic space robots in [22]. Path planning for space manipulators which contain nonholonomic behavior was presented in [23]. These applications were restricted to certain kinds of field robots such as unmanned aerial vehicles [24], snake-like robots [25], unmanned ground vehicles [8], the human–robot interaction system [27] and crawling robots [28]. One may compare link WIP systems with the cart and pendulum systems [29], which seems quite similar at the first glance. However, there are major distinctions between these two kinds of systems, e.g., WIP system is driven by two wheels and its motion is not only on the horizontal plane but also on the vertical plane. In addition,

R. Cui (✉) · Z. Mao
School of Marine Science and Technology, Northwestern
Polytechnical University, Xi'an 710072,
People's Republic of China
e-mail: rongxin.cui@gmail.com

J. Guo
College of Physics and Electrical Engineering, Anyang Normal
University, Anyang 455000, People's Republic of China

the motors that drive the wheels are mounted on the pendulum body directly [5], while the actuator does not directly drive the pendulum in the cart.

For the control of WIP system, numerous existing control designs are based on the model linearization. A linear robust controller for the WIP system was presented in [30], where the yaw angle was not considered in the control design. A linear controller based on the planar model was developed in [31]. Furthermore, the feedback linearization method has also been employed in the WIP control in [5], where the position controller is designed based on a two-level velocity control. These linear model-based design may ignore some nonlinearities of the WIP system in the practical applications. In addition, there are always some model parameters of the WIP system with uncertainties, e.g., the rider's mass is not available for the control design and can be changed from time to time. To overcome these challenges, fuzzy approximation-based control was proposed for the WIP in [11, 15, 16], where the control is designed directly based on the nonlinear model. In fact, fuzzy approximation or the neural network approximation-based nonlinear control have been widely used in the control of system with uncertainties and unknown disturbances [32, 32–37]. The representative works on the WIP control are [1, 15, 16, 38, 39]. A novel adaptive robust motion control considering the parametric and functional model uncertainties of WIP was presented in [38], where the output error of the WIP converges to a neighborhood of zero. In [1], a recurrent cerebellar model articulation control was proposed for the WIP, where the output feedback case is considered. Sliding mode-based control for the velocity tracking of the WIP systems was presented in [9]. Other recurrent cerebellar model articulation-based controls for WIP were reported in [40, 41], where the basic idea is the same as the neural network-based intelligent control while the model uncertainties and external disturbances estimated along with the control design [26]. An output feedback adaptive neural network (NN)-based adaptive control was proposed for the WIP system in [7], where a linear dynamic compensator is employed. Both the stable dynamic balance and the trajectory tracking of the WIP system are achieved in [7].

Motivated by [16, 38], we design the controller for the WIP based on the nonlinear model derived by Lagrangian approach in this paper. Through a coordinate transformation, we divide the system into three sub-systems and employ the backstepping method to

design the adaptive control for each sub-system individually. The remainder of this work is organized as follows. Some preliminaries and the problem formulation are introduced in Sect. 2. The adaptive backstepping control design is presented in Sect. 3, followed by the simulation studies in Sect. 4. Conclusions and remarks are drawn in Sect. 5.

2 System description

In this work, the dynamics of the WIP model is described as follows [10].

$$M(q)\ddot{q} + V(q, \dot{q})\dot{q} + F(\dot{q}) + G(q) + D = B(q)\tau + f \quad (1)$$

where $q \in \mathbb{R}^4$ is the generalized coordinates vector and $q_1 = x$, $q_2 = y$, $q_3 = \theta$ and $q_4 = \alpha$. The definitions of the symbols are shown in Table 1.

Define $q = [q_v^T, \alpha]^T$, where the new vector $q_v = [x, y, \theta]^T$, we have

$$\begin{aligned} M(q) &= \begin{bmatrix} M_v & M_{v\alpha} \\ M_{\alpha v} & M_\alpha \end{bmatrix}, V(q, \dot{q}) = \begin{bmatrix} V_v & V_{v\alpha} \\ V_{\alpha v} & V_\alpha \end{bmatrix}, \\ G(q) &= \begin{bmatrix} G_v \\ G_\alpha \end{bmatrix}, F(\dot{q}) = \begin{bmatrix} f_v \\ f_\alpha \end{bmatrix}, D = \begin{bmatrix} d_v \\ d_\alpha \end{bmatrix} \\ B(q) &= \begin{bmatrix} B_v & 0 \\ 0 & B_\alpha \end{bmatrix}, \tau = \begin{bmatrix} \tau_v \\ 0 \end{bmatrix}, \end{aligned}$$

In this work, we consider that the WIP system is subjected to the nonholonomic constraints. In practical applications, we can adopt the approach that produce sufficient frictions between the wheels of the platform and the ground. In such case, we can assume that the nonholonomic constraints are available for the control design. In addition, due to the fact that the angular displacements of the wheels can be represented by the position coordinates x and y , it is reasonable to use x and y as the generalized coordinates for the WIP system.

2.1 Reduced dynamics

Define J_v as the nonholonomic constraints-related kinematic constraint matrix, the nonholonomic constraints on the vehicles can be described as [10]

$$J_v \dot{q}_v = 0 \quad (2)$$

Table 1 Nomenclature

Symbol	Description
$x, y \in \mathbb{R}$	Mid-point position of the two driving wheels
$\theta \in \mathbb{R}$	Heading angle in the fixed frame
$\alpha \in \mathbb{R}$	Tilt angle in the fixed frame
$M(q) \in \mathbb{R}^{4 \times 4}$	Inertia matrix
$V(q, \dot{q}) \in \mathbb{R}^4$	Coriolis and centrifugal forces vector
$F(\dot{q}) \in \mathbb{R}^4$	Friction forces vector
$G(q) \in \mathbb{R}^4$	Gravitational forces vector
$B(q) \in \mathbb{R}^{4 \times 3}$	Control coefficients matrix
$\tau \in \mathbb{R}^3$	Control inputs vector
$f = J^T \lambda \in \mathbb{R}^4$	Constraint forces vector
$J^T \in \mathbb{R}^4$	Jacobian matrix
$\lambda \in \mathbb{R}$	Lagrangian multipliers
$M_v \in \mathbb{R}^{3 \times 3}$	Mobile platform Inertia matrix
$M_\alpha \in \mathbb{R}$	Inverted pendulum inertia matrix
$M_{v\alpha} \in \mathbb{R}^{3 \times 1}$	Mobile platform coupling inertia matrix
$M_{\alpha v} \in \mathbb{R}^{1 \times 3}$	Inverted pendulum coupling inertia matrix
$V_v \in \mathbb{R}^{3 \times 3}$	Mobile platform Coriolis and Centripetal torques
$V_\alpha \in \mathbb{R}$	Inverted pendulum Coriolis and Centripetal torques
$V_{v\alpha} \in \mathbb{R}^{3 \times 1}$	Mobile platform Coupling Centripetal and Coriolis torques
$V_{\alpha v} \in \mathbb{R}^{1 \times 3}$	Inverted pendulum Coupling Centripetal and Coriolis torques
$G_v \in \mathbb{R}^{3 \times 1}$	Mobile platform Gravitational torque vectors
$G_\alpha \in \mathbb{R}$	Inverted pendulum Gravitational torque vectors
$\tau_v \in \mathbb{R}^{3 \times 1}$	Mobile platform Control input vector
$f_v(t) \in \mathbb{R}^{3 \times 1}$	Friction force on the mobile platform
$f_\alpha(t) \in \mathbb{R}$	Friction force on the inverted pendulum
$d_v(t) \in \mathbb{R}^{3 \times 1}$	Disturbances on the mobile platform
$d_\alpha(t) \in \mathbb{R}$	Disturbances on the inverted pendulum
$\omega \in \mathbb{R}$	Angular velocity of the platform
$v \in \mathbb{R}$	Heading velocity of the platform

The constraints can be written as $\Omega_n = \{(q_v, \dot{q}_v) | J_v \dot{q}_v = 0\}$, which means a restriction of the dynamics on the manifold Ω_n is added.

It is possible to find a full rank matrix $\Phi = [\Phi_1(q), \Phi_2(q)] \in R^{3 \times 2}$, where $\Phi_1(q)$ and $\Phi_2(q)$ are linearly independent smooth vector fields satisfying $\Phi^T J_v^T = 0$ [39]. In detail, $J_v = [0, \sin(\theta), -\cos(\theta)]$ and Φ can be written as

$$\Phi = \begin{bmatrix} 1 & 0 \\ 0 & \cos(\theta) \\ 0 & \sin(\theta) \end{bmatrix} \tag{3}$$

Now we can define a new vector $\dot{\eta} = [\omega, v]^T \in \mathbb{R}^2$, and thus have

$$\dot{q}_v = \Phi(q) \dot{\eta}. \tag{4}$$

Define $\zeta = [\eta^T, \alpha]^T$, we have $\dot{\zeta} = [\omega, v, \dot{\alpha}]^T$, i.e., $\dot{\zeta}_1 = \omega$, $\dot{\zeta}_2 = v$, and $\dot{\zeta}_3 = \dot{\alpha}$. Define a new matrix

$$\bar{\Phi} = \text{diag}[\Phi^T, I] = \begin{bmatrix} 1 & 0 & 0 & 0 \\ 0 & \cos \theta & \sin \theta & 0 \\ 0 & 0 & 0 & 1 \end{bmatrix},$$

while both sides of (1) multiply by $\bar{\Phi}, J_v^T$ will be eliminated. Then, we can write the WIP dynamics as

$$M_1(\zeta) \ddot{\zeta} + V_1(\zeta, \dot{\zeta}) \dot{\zeta} + F_1(\dot{\zeta}) + G_1(\zeta) + D_1 = B_1 \tau \tag{5}$$

where

$$M_1(\zeta) = \begin{bmatrix} \Phi^T M_v \Phi & \Phi^T M_{v\alpha} \\ M_{\alpha v} \Phi & M_\alpha \end{bmatrix},$$

$$V_1(\zeta, \dot{\zeta}) = \begin{bmatrix} \Phi^T M_v \dot{\Phi} + \Phi^T V_v \Phi & \Phi^T V_{v\alpha} \\ M_{\alpha v} \dot{\Phi} + V_{\alpha v} \Phi & V_\alpha \end{bmatrix},$$

$$G_1(\zeta) = \begin{bmatrix} \Phi^T G_v \\ G_\alpha \end{bmatrix}, F_1(\dot{\zeta}) = \begin{bmatrix} \Phi^T F_v \\ F_\alpha \end{bmatrix},$$

$$D_1 = \begin{bmatrix} \Phi^T d_v \\ d_\alpha \end{bmatrix}, B_1 \tau = \begin{bmatrix} \Phi^T B_v \tau_v \\ 0 \end{bmatrix}.$$

Similar to [16], the control objective of this work can be formulated as follows. Designing a control for the WIP system ensures that $|\zeta_1(t) - \zeta_{1d}(t)| \leq \epsilon_1$, $|\zeta_3(t) - \zeta_{3d}(t)| \leq \epsilon_3$, $t \rightarrow \infty$, where $\zeta_{1d}(t)$ and $\zeta_{3d}(t)$ are the desired trajectories for $\zeta_1(t)$ and $\zeta_3(t)$, respectively, and $\epsilon_j > 0$, $j = 1, 3$ are small constants. In the meantime, all the closed-loop signals of the system must be bounded. Without loss of generality, it is assumed that $\zeta_{1d}(t)$, $\zeta_{3d}(t)$ and whose time derivatives up to the third order are bounded and continuously differentiable.

Remark 1 In this paper, it is expected to maintain $\zeta_{3d} = 0$ and $\dot{\zeta}_{3d} = 0$ for the WIP.

Assumption 1 The friction force, $F_1(\dot{\zeta}) = [f_1, f_2, f_3]^T$, acts on each vector independently, and it is a function of the velocity. F_1 can be written as $F_1(\dot{\zeta}) = \mathcal{B} \dot{\zeta}$, where \mathcal{B} is a positive definite diagonal matrix.

2.2 System transformation

According to the structure of the dynamics of the WIP system, we have

$$\begin{aligned}
 M_1(\zeta) &= \begin{bmatrix} m_{11}(\zeta_3) & 0 & 0 \\ 0 & m_{22} & m_{23}(\zeta_3) \\ 0 & m_{23}(\zeta_3) & m_{33} \end{bmatrix}, \\
 V_1(\zeta, \dot{\zeta}) &= \begin{bmatrix} v_{11} & 0 & v_{13} \\ 0 & 0 & v_{23} \\ v_{31} & 0 & 0 \end{bmatrix} \\
 F_1(\dot{\zeta}) &= \begin{bmatrix} f_1 \\ f_2 \\ f_3 \end{bmatrix}, D_1 = \begin{bmatrix} d_1 \\ d_2 \\ 0 \end{bmatrix}, G_1(\zeta) = \begin{bmatrix} g_1(\zeta) \\ g_2(\zeta) \\ g_3(\zeta) \end{bmatrix}, \\
 B_1 \tau &= \begin{bmatrix} \tau_1 \\ \tau_2 \\ 0 \end{bmatrix} \tag{6}
 \end{aligned}$$

where m_{22} and m_{33} are unknown constants, $m_{11}(\zeta_3)$, $m_{23}(\zeta_3)$, v_{11} , v_{13} , v_{23} , v_{31} , f_i , $g_i(\zeta)$, $i = 1, \dots, 3$, and d_1, d_2 are unknown continuous functions.

Property 1 From (6), we can find that both m_{12} and m_{13} are all zero in the inertia matrix $M_1(\zeta)$, this is because the vertical inertia and the rotational inertia are decoupled with respected to the vertical axis. In addition, both $m_{11}(\zeta_3)$ and $\frac{m_{22}m_{33}-m_{23}^2(\zeta_3)}{m_{33}}$ are positive due to the positive definite of $M_1(\zeta)$. $\dot{M}_1 - 2V_1$ is skew-symmetric, which follows that $\frac{d}{dt}(m_{11}(\zeta_3)) - 2v_{11} = 0$.

Remark 2 From the Lagrangian formulation, we know that v_{23} is relevant to $\sin(\zeta_3)$ and $\dot{\zeta}_3$, and v_{31} is relevant to $\sin(2\zeta_3)$.

It is clear that $\ddot{\zeta}_2$ and $\ddot{\zeta}_3$ are coupled from (1) and (6). Thus, it is difficult to design the controller based on (1) directly. By using the physical properties of the WIP model and a simple transformation of (6), three subsystems, namely ζ_1 -subsystem, ζ_2 -subsystem, and ζ_3 -subsystem can be obtained, which can be described as follows [42].

$$m_{11}(\zeta_3)\ddot{\zeta}_1 + v_{11}\dot{\zeta}_1 + v_{13}\dot{\zeta}_3 + g_1 + f_1 + d_1 = \tau_1 \tag{7}$$

$$\begin{aligned}
 &\frac{m_{22}m_{33}-m_{23}^2(\zeta_3)}{m_{33}}\ddot{\zeta}_2 + v_{23}\dot{\zeta}_3 \\
 &+ \frac{m_{23}(\zeta_3)}{m_{33}}(-v_{31}\dot{\zeta}_1 - f_3 - g_3) + d_2 + f_2 + g_2 = \tau_2 \tag{8}
 \end{aligned}$$

$$\begin{aligned}
 &\frac{m_{22}m_{33}-m_{23}^2(\zeta_3)}{m_{22}}\ddot{\zeta}_3 + v_{31}\dot{\zeta}_1 + f_3 + g_3 \\
 &+ \frac{m_{23}(\zeta_3)}{m_{22}}(\tau_2 - v_{23}\dot{\zeta}_3 - d_2 - f_2 - g_2) = 0 \tag{9}
 \end{aligned}$$

From the above equations, we can further have

$$m_{11}(\zeta_3)\ddot{\zeta}_1 + v_{11}\dot{\zeta}_1 + v_{13}\dot{\zeta}_3 + g_1 + f_1 + d_1 = \tau_1 \tag{10}$$

$$\begin{aligned}
 &\frac{m_{22}m_{33}-m_{23}^2(\zeta_3)}{m_{33}}\ddot{\zeta}_2 - \frac{m_{23}(\zeta_3)}{m_{33}}(v_{31}\dot{\zeta}_1 + f_3 + g_3) \\
 &- (\tau_2 - v_{23}\dot{\zeta}_3 - d_2 - f_2 - g_2) = 0 \tag{11}
 \end{aligned}$$

$$\begin{aligned}
 &\frac{m_{22}m_{33}-m_{23}^2(\zeta_3)}{m_{23}(\zeta_3)}\ddot{\zeta}_3 - v_{23}\dot{\zeta}_3 \\
 &+ \frac{m_{22}}{m_{23}(\zeta_3)}(v_{31}\dot{\zeta}_1 + f_3 + g_3) - (f_2 + g_2 + d_2) = -\tau_2 \tag{12}
 \end{aligned}$$

Define $x_1 = \zeta_1, x_2 = \dot{\zeta}_1, x_3 = \zeta_3$, and $x_4 = \dot{\zeta}_3$, then Eqs. (10) and (11) can be transformed into a general form as below:

$$\dot{x}_1 = x_2 \tag{13}$$

$$\begin{aligned}
 \dot{x}_2 &= -\frac{v_{11}}{m_{11}(x_3)}x_2 - \frac{v_{13}}{m_{11}(x_3)}x_4 \\
 &- \frac{g_1}{m_{11}(x_3)} - \frac{f_1}{m_{11}(x_3)} \\
 &- \frac{d_1}{m_{11}(x_3)} + \frac{1}{m_{11}(x_3)}\tau_1 \tag{14}
 \end{aligned}$$

$$\dot{x}_3 = x_4 \tag{15}$$

$$\begin{aligned}
 \dot{x}_4 &= \frac{m_{23}(x_3)}{m_{22}m_{33}-m_{23}^2(x_3)}v_{23}x_4 \\
 &- \frac{m_{22}}{m_{22}m_{33}-m_{23}^2(x_3)}(v_{31}x_2 + f_3 + g_3) \\
 &+ \frac{m_{23}(x_3)}{m_{22}m_{33}-m_{23}^2(x_3)}(f_2 + g_2 + d_2) \\
 &- \frac{m_{23}(x_3)}{m_{22}m_{33}-m_{23}^2(x_3)}\tau_2 \tag{16}
 \end{aligned}$$

We put the nonlinear parts $h_1(\zeta, \dot{\zeta}, t) = v_{11}\dot{\zeta}_1 + v_{13}\dot{\zeta}_3 + g_1 + f_1 + d_1$ in (14) and $h_2(\zeta, \dot{\zeta}, t) = m_{23}v_{23}\dot{\zeta}_3 - m_{22}(v_{31}\dot{\zeta}_1 + f_3 + g_3) + m_{23}(f_2 + g_2 + d_2)$ in (16) into a parameterized formulation as follows.

$$h_1(\zeta, \dot{\zeta}, t) = \theta_1^T \Psi_1(\zeta, \dot{\zeta}) \tag{17}$$

$$h_2(\zeta, \dot{\zeta}, t) = \theta_2^T \Psi_2(\zeta, \dot{\zeta}) \tag{18}$$

where $\theta_i, i = 1, 2$ is the uncertain parameter vector needs to be estimated, and $\Psi_i(\zeta, \dot{\zeta}), i = 1, 2$ is the regressor matrix depending on $\zeta = [\zeta_1, \zeta_2, \zeta_3]^T$ and $\dot{\zeta} = [\dot{\zeta}_1, \dot{\zeta}_2, \dot{\zeta}_3]^T$.

3 Adaptive backstepping control design

We develop a backstepping-based adaptive control for the WIP system with parameter uncertainties in this section. As one of the most popular design methods

for the nonlinear system control design, backstepping has been widely used in the robot control, and in the control of manipulators. To facility the control design, we first change the coordinates of the system.

3.1 ζ_1 -Subsystem

Step 1. Define the error $z_1(t) = x_1(t) - \zeta_{1d}(t)$. Its derivative can be written as

$$\dot{z}_1(t) = z_2(t) + \alpha_1(t) \tag{19}$$

where $z_2(t) = x_2(t) - \dot{\zeta}_{1d}(t) - \alpha_1(t)$, $\alpha_1(t)$ is a virtual control to be defined as

$$\alpha_1(t) = -c_1 z_1(t) \tag{20}$$

where $c_1 \in \mathbb{R}^+$. For concise, we omit the t for the variables. Substituting (20) into (19), we have

$$\dot{z}_1 = z_2 - c_1 z_1 \tag{21}$$

To stabilize the z_1 subsystem (19), following Lyapunov function candidate is chosen.

$$V_1 = \frac{1}{2} z_1^2 \tag{22}$$

The time derivative of V_1 along the solution of (21) can be written as

$$\dot{V}_1 = z_1 \dot{z}_1 = z_1 (z_2 + \alpha_1) = z_1 z_2 + z_1 \alpha_1 \tag{23}$$

The closed-loop form of (23) with (20) is given by

$$z_1 \dot{z}_1 = -c_1 z_1^2 + z_1 z_2 \tag{24}$$

Step 2. The derivative of $z_2 = x_2 - \dot{\zeta}_{1d} - \alpha_1$ can be described as

$$\dot{z}_2 = \frac{1}{m_{11}} (\tau_1 - h_1) - \ddot{\zeta}_{1d} - \dot{\alpha}_1 \tag{25}$$

Now we select the control as follows.

$$\tau_1 = \hat{m}_{11} \bar{\tau}_1 + \hat{h}_1 \tag{26}$$

$$\bar{\tau}_1 = -c_2 z_2 - z_1 + \ddot{\zeta}_{1d} + \dot{\alpha}_1 \tag{27}$$

where $c_2 \in \mathbb{R}^+$, \hat{m}_{11} and \hat{h}_1 are the estimates of unknown items m_{11} and h_1 , respectively.

Substituting (26) into (25), we have

$$\dot{z}_2 = \frac{1}{m_{11}} \hat{m}_{11} \bar{\tau}_1 + \frac{1}{m_{11}} (\hat{h}_1 - h_1) - \ddot{\zeta}_{1d} - \dot{\alpha}_1 \tag{28}$$

Theorem 1 For the closed-loop system consisting of system dynamics (1), and the control law (26), we choose the updated law of $\hat{\theta}_1$ and \hat{m}_{11} as

$$\dot{\hat{\theta}}_1 = -\Gamma \Psi_1 z_2 \tag{29}$$

$$\dot{\hat{m}}_{11} = -\gamma \bar{\tau}_1 z_2 \tag{30}$$

where $\gamma \in \mathbb{R}^+$ and $\Gamma = \Gamma^T > 0$ are designed parameters, $\hat{\theta}_1$ is the estimation of the unknown parameter θ_1 . Then, $z_1 = 0$ will be a globally uniformly stable equilibrium of the closed-loop system. This ensures the global boundedness of the state x_1 , the parameter estimation $\hat{\theta}_1$, \hat{m}_{11} , and the control τ_1 , and $\lim_{t \rightarrow \infty} z_1(t) = 0$, i.e., $\lim_{t \rightarrow \infty} [\zeta_1(t) - \zeta_{1d}(t)] = 0$

Proof Select the following Lyapunov function candidate.

$$V_2 = \frac{1}{2} z_1^2 + \frac{1}{2} z_2^2 + \frac{1}{2m_{11}} \tilde{\theta}_1^T \Gamma^{-1} \tilde{\theta}_1 + \frac{1}{2\gamma m_{11}} \tilde{m}_{11}^2 \tag{31}$$

where $\tilde{m}_{11} = m_{11} - \hat{m}_{11}$, $\tilde{\theta}_1 = \theta_1 - \hat{\theta}_1$. The time derivative of V_1 along (24) and (28) can be written as

$$\begin{aligned} \dot{V}_2 &= z_1 \dot{z}_1 + z_2 \dot{z}_2 + \frac{1}{m_{11}} \tilde{\theta}_1^T \Gamma^{-1} \dot{\tilde{\theta}}_1 + \frac{1}{\gamma m_{11}} \tilde{m}_{11} \dot{\tilde{m}}_{11} \\ &= -c_1 z_1^2 + z_2 \left(\frac{1}{m_{11}} (\tau_1 - h_1) + z_1 - \ddot{\zeta}_{1d} - \dot{\alpha}_1 \right) \\ &\quad + \frac{1}{m_{11}} \tilde{\theta}_1^T \Gamma^{-1} \dot{\tilde{\theta}}_1 + \frac{1}{\gamma m_{11}} \tilde{m}_{11} \dot{\tilde{m}}_{11} \\ &= -c_1 z_1^2 + z_2 \left(\frac{1}{m_{11}} (\tau_1 - h_1) - c_2 z_2 - \bar{\tau}_1 \right) \\ &\quad + \frac{1}{m_{11}} \tilde{\theta}_1^T \Gamma^{-1} \dot{\tilde{\theta}}_1 + \frac{1}{\gamma m_{11}} \tilde{m}_{11} \dot{\tilde{m}}_{11} \\ &= -c_1 z_1^2 - c_2 z_2^2 + z_2 \left(\frac{1}{m_{11}} (\hat{m}_{11} \bar{\tau}_1 + \hat{h}_1 - h_1) - \bar{\tau}_1 \right) \\ &\quad + \frac{1}{m_{11}} \tilde{\theta}_1^T \Gamma^{-1} \dot{\tilde{\theta}}_1 + \frac{1}{\gamma m_{11}} \tilde{m}_{11} \dot{\tilde{m}}_{11} \\ &= -c_1 z_1^2 - c_2 z_2^2 + \frac{1}{m_{11}} z_2 \left(-\tilde{m}_{11} \bar{\tau}_1 - \tilde{\theta}_1^T \Psi_1 \right) \\ &\quad + \frac{1}{m_{11}} \tilde{\theta}_1^T \Gamma^{-1} \dot{\tilde{\theta}}_1 + \frac{1}{\gamma m_{11}} \tilde{m}_{11} \dot{\tilde{m}}_{11} \end{aligned} \tag{32}$$

Due to the fact that $\dot{\hat{\theta}}_1 = -\dot{\theta}_1$, and $\dot{\hat{m}}_{11} = -\dot{m}_{11}$, we have

$$\begin{aligned} \dot{V}_2 &= -c_1 z_1^2 - c_2 z_2^2 - \frac{1}{m_{11}} \tilde{m}_{11} (z_2 \bar{\tau}_1 + \frac{1}{\gamma} \dot{\hat{m}}_{11}) \\ &\quad - \frac{1}{m_{11}} \tilde{\theta}_1^T (\Psi_1 z_2 + \Gamma^{-1} \dot{\hat{\theta}}_1) \\ &= -c_1 z_1^2 - c_2 z_2^2 \end{aligned} \tag{33}$$

The error Eq.(28) is corresponding to the closed-loop system. It consists of plant dynamics (1), the parameter update laws (29), (30), and the control (26). The time derivation of (31) along the (24) and (28) results in (33), which implies the globally uniformly stable of the equilibrium $z_1 = 0$. \square

From Eqs.(31) and (33), we can conclude that $\tilde{\theta}_1$ and \tilde{m}_{11} are bounded. we can find that x_1 is also bound due to the boundedness of z_1 and ζ_{1d} . The boundedness of x_1 follows from the boundedness of α_1 , which is defined in (20) and ζ_{1d} , i.e., $x_2 = z_2 - \dot{\zeta}_{1d} - \alpha_1$. Therefore, τ_1 is bounded according to (26) because of the boundedness of $z_1, z_2, \hat{\theta}_1$, and \hat{m}_{11} . Using the LaSalle–Yoshizawa theorem [43], we can obtain $z_i(t) \rightarrow 0, i = 1, 2, t \rightarrow \infty$, which implies that $\lim_{t \rightarrow \infty} [\zeta_1(t) - \zeta_{1d}(t)] = 0$.

According to (33), V_2 is nonincreasing, then we have

$$\begin{aligned} \|z_1\|_2^2 &= \int_0^\infty |z_1(\tau)|^2 d\tau \leq \frac{1}{c_1} [V_2(0) - V_2(\infty)] \\ &\leq \frac{1}{c_1} V_2(0) \end{aligned} \tag{34}$$

Therefore,

$$V_2(0) = \frac{1}{2m_{11}} \tilde{\theta}_1^T(0) \Gamma^{-1} \tilde{\theta}_1(0) + \frac{1}{2\gamma m_{11}} \tilde{m}_{11}(0)^2 \tag{35}$$

where $z_1(0) = z_2(0) = 0, \gamma$, and Γ are decreasing functions independent of c_1 . Then, we can obtain the bounds from (34) and (35) as

$$\|z_1\|_2 \leq \frac{1}{\sqrt{c_1}} \sqrt{V_2(0)} \tag{36}$$

It is clear that this bound can be reduced either increasing c_1 or increasing γ and Γ simultaneously. From (20) and (19), we have

$$\|\dot{x}_1 - \dot{\zeta}_{1d}\|_2 = \|z_2 - c_1 z_1\|_2 \leq \|z_2\|_2 + c_1 \|z_1\|_2 \tag{37}$$

Similarly, $\|z_2\|_2 \leq \frac{1}{\sqrt{c_1} \sqrt{V_2(0)}}$ can be obtained. Along with (36), we have

$$\begin{aligned} \|\dot{x}_1 - \dot{\zeta}_{1d}\|_2 &\leq \left(\frac{1}{\sqrt{c_1}} + \sqrt{c_1} \right) \\ &\quad \times \sqrt{\frac{1}{2m_{11}} \tilde{\theta}_1^T(0) \Gamma^{-1} \tilde{\theta}_1(0) + \frac{1}{2\gamma m_{11}} \tilde{m}_{11}(0)^2} \end{aligned} \tag{38}$$

Remark 3 The following conclusions can be made based on (1):

- (i) For any positive design parameters c_1, c_2, γ , and Γ , the signals are guaranteed to be globally and uniformly bounded. For the control design, the priori information of the parameter uncertainties is not required.
- (ii) To improve the tracking performance, c_1 maybe increased. However, this may result in large velocity tracking error. The small velocity tracking error can be achieved after fixing c_1 to some acceptable value and increasing c_2, γ , or Γ simultaneously.

3.2 ζ_3 -Subsystem

Step 1. Define an error variable $z_3 = x_3 - \zeta_{3d}$, whose time derivative can be written as

$$\dot{z}_3 = z_4 + \alpha_2 \tag{39}$$

where $z_4 = x_4 - \dot{\zeta}_{3d} - \alpha_2, \alpha_2$ is a virtual control defined as

$$\alpha_2 = -c_3 z_3 \tag{40}$$

where $c_3 \in \mathbb{R}^+$ is a constant. Substituting (40) into (39), we have

$$\dot{z}_3 = z_4 - c_3 z_3 \tag{41}$$

To stabilize z_3 , we select the following Lyapunov function candidate.

$$V_3 = \frac{1}{2} z_3^2 \tag{42}$$

The derivative of V_3 along the solution of (41) can be described as

$$\dot{V}_3 = z_3 \dot{z}_3 = z_3 (z_4 + \alpha_2) = z_3 z_4 + z_3 \alpha_2 \tag{43}$$

The closed-loop form of (43) with (40) is given by

$$z_3 \dot{z}_3 = -c_3 z_3^2 + z_3 z_4 \tag{44}$$

Step 2. The time derivative of $z_4 = x_4 - \dot{\zeta}_{3d} - \alpha_2$ can be written as

$$\dot{z}_4 = \frac{1}{\varpi} (h_2 - \tau_2) - \ddot{\zeta}_{3d} - \dot{\alpha}_2 \tag{45}$$

where $\varpi = \frac{m_{22}m_{33} - m_{23}^2(\zeta_3)}{m_{23}(\zeta_3)}$.

We design the following controller.

$$\tau_2 = \hat{\varpi} \bar{\tau}_2 + \hat{h}_2 \tag{46}$$

$$\bar{\tau}_2 = c_4 z_4 + z_3 - \ddot{\zeta}_{3d} - \dot{\alpha}_2 \tag{47}$$

where $c_4 \in \mathbb{R}^+$ is a designed constant, $\hat{\varpi}$ and \hat{h}_2 are the estimates of the unknown parameters ϖ and h_2 , respectively. Substituting (46) into (45), we have

$$\dot{z}_4 = -\frac{1}{\varpi} \hat{\varpi} \bar{\tau}_2 + \frac{1}{\varpi} (h_2 - \hat{h}_2) - \ddot{\zeta}_{3d} - \dot{\alpha}_2 \tag{48}$$

Theorem 2 For the closed-loop system consisting of system dynamics (1), and the control law (46), we choose the parameter update law as

$$\dot{\hat{\theta}}_2 = \Lambda \Psi_2 z_4 \tag{49}$$

$$\dot{\hat{\varpi}} = \lambda \bar{\tau}_2 z_4 \tag{50}$$

where $\lambda \in \mathbb{R}^+$ is a designed constant, and $\hat{\theta}_2$ is the estimates of unknown parameter θ_2 . $\Lambda = \Lambda^T > 0$ is a dimensionally compatible constant matrix. Then $z_3 = 0$ will be a globally uniformly stable equilibrium of the closed-loop system. It follows that x_3 , τ_2 , $\hat{\theta}_2$, and $\hat{\varpi}$ are bounded, and $\lim_{t \rightarrow \infty} z_3(t) = 0$, i.e., $\lim_{t \rightarrow \infty} [\zeta_3(t) - \zeta_{3d}(t)] = 0$.

Proof Select the following Lyapunov function candidate.

$$V_4 = \frac{1}{2} z_3^2 + \frac{1}{2} z_4^2 + \frac{1}{2\varpi} \tilde{\theta}_2^T \Lambda^{-1} \tilde{\theta}_2 + \frac{1}{2\lambda\varpi} \tilde{\varpi}^2 \tag{51}$$

where $\tilde{\varpi} = \varpi - \hat{\varpi}$, $\tilde{\theta}_2 = \theta_2 - \hat{\theta}_2$. The time derivative of V_3 along (44) and (48) can be written as

$$\begin{aligned} \dot{V}_2 &= z_3 \dot{z}_3 + z_4 \dot{z}_4 + \frac{1}{\varpi} \tilde{\theta}_2^T \Lambda^{-1} \dot{\tilde{\theta}}_2 + \frac{1}{\lambda\varpi} \tilde{\varpi} \dot{\tilde{\varpi}} \\ &= -c_3 z_3^2 + z_4 \left(\frac{1}{\varpi} (h_2 - \tau_2) + z_3 - \ddot{\zeta}_{3d} - \dot{\alpha}_2 \right) \\ &\quad + \frac{1}{\varpi} \tilde{\theta}_2^T \Lambda^{-1} \dot{\tilde{\theta}}_2 + \frac{1}{\lambda\varpi} \tilde{\varpi} \dot{\tilde{\varpi}} \\ &= -c_3 z_3^2 + z_4 \left(\frac{1}{\varpi} (h_2 - \tau_2) - c_4 z_4 + \bar{\tau}_2 \right) \end{aligned}$$

$$\begin{aligned} &+ \frac{1}{\varpi} \tilde{\theta}_2^T \Lambda^{-1} \dot{\tilde{\theta}}_2 + \frac{1}{\lambda\varpi} \tilde{\varpi} \dot{\tilde{\varpi}} \\ &= -c_3 z_3^2 - c_4 z_4^2 + z_4 \left(\frac{1}{\varpi} (-\hat{\varpi} \bar{\tau}_2 + h_2 - \hat{h}_2) + \bar{\tau}_2 \right) \\ &\quad + \frac{1}{\varpi} \tilde{\theta}_2^T \Lambda^{-1} \dot{\tilde{\theta}}_2 + \frac{1}{\lambda\varpi} \tilde{\varpi} \dot{\tilde{\varpi}} \\ &= -c_3 z_3^2 - c_4 z_4^2 + \frac{1}{\varpi} z_4 (\tilde{\varpi} \bar{\tau}_2 + \tilde{\theta}_2^T \Psi_2) \\ &\quad + \frac{1}{\varpi} \tilde{\theta}_2^T \Lambda^{-1} \dot{\tilde{\theta}}_2 + \frac{1}{\lambda\varpi} \tilde{\varpi} \dot{\tilde{\varpi}} \tag{52} \end{aligned}$$

Since $\dot{\tilde{\theta}}_2 = -\dot{\hat{\theta}}_2$, and $\dot{\tilde{\varpi}} = -\dot{\hat{\varpi}}$, we have

$$\begin{aligned} \dot{V}_4 &= -c_3 z_3^2 - c_4 z_4^2 + \frac{1}{\varpi} \tilde{\varpi} (z_4 \bar{\tau}_2 - \frac{1}{\lambda} \dot{\tilde{\varpi}}) \\ &\quad + \frac{1}{\varpi} \tilde{\theta}_2^T (\Psi_2 z_4 - \Lambda^{-1} \dot{\tilde{\theta}}_2) \\ &= -c_3 z_3^2 - c_4 z_4^2 \tag{53} \end{aligned}$$

The error Eq.(48) corresponds to the closed-loop system, which consists of plant dynamics (1), the parameter update laws (49), (50), and the controller (46). The time derivative of Lyapunov function (51) along (44) and (48) results in (53), which implies the globally uniformly stable of the equilibrium $z_3 = 0$. \square

From Eqs.(51) and (53), we can conclude that $\tilde{\theta}_2$ and $\tilde{\varpi}$ are bounded. x_3 is also bounded due to the boundedness of $z_3 = x_3 - \zeta_{3d}$ and ζ_{3d} . It follows that α_2 is bounded, which is defined in (40) and ζ_{3d} , i.e., $x_4 = z_4 - \dot{\zeta}_{3d} - \alpha_2$. Therefore, τ_2 is bounded because of the boundedness of z_3 , z_4 , $\hat{\theta}_2$, and $\hat{\varpi}$. By applying the LaSalle-Yoshizawa theorem [43], we have $z_i(t) \rightarrow 0$, $i = 3, 4$, $t \rightarrow \infty$, which implies that $\lim_{t \rightarrow \infty} [\zeta_3(t) - \zeta_{3d}(t)] = 0$.

From (53), we can find that V_4 is nonincreasing, then

$$\begin{aligned} \|z_3\|_2^2 &= \int_0^\infty |z_3(\tau)|^2 d\tau \leq \frac{1}{c_3} [V_4(0) - V_4(\infty)] \\ &\leq \frac{1}{c_3} V_4(0) \tag{54} \end{aligned}$$

Therefore, we have

$$V_4(0) = \frac{1}{2\varpi} \tilde{\theta}_2^T(0) \Lambda^{-1} \tilde{\theta}_2(0) + \frac{1}{2\lambda\varpi} \tilde{\varpi}(0)^2 \tag{55}$$

where $z_3(0) = z_4(0) = 0$, λ , and Λ are decreasing functions independent of c_3 . This implies that the bounds

$$\|z_3\|_2 \leq \frac{1}{\sqrt{c_3}} \sqrt{V_4(0)} \tag{56}$$

can be asymptotically reduced either increasing c_3 or increasing λ and Λ simultaneously. From (39) and (40), we have

$$\|\dot{x}_3 - \dot{\zeta}_{3d}\|_2 = \|z_4 - c_3 z_3\|_2 \leq \|z_4\|_2 + c_3 \|z_3\|_2 \quad (57)$$

Similarly, $\|z_4\|_2 \leq \frac{1}{\sqrt{c_3} \sqrt{V_4(0)}}$ can be obtained. Along with (56), we have

$$\begin{aligned} \|\dot{x}_3 - \dot{\zeta}_{3d}\|_2 &\leq \left(\frac{1}{\sqrt{c_3}} + \sqrt{c_3} \right) \\ &\times \sqrt{\frac{1}{2\varpi} \tilde{\theta}_2^T(0) \Lambda^{-1} \tilde{\theta}_2(0) + \frac{1}{2\lambda\varpi} \tilde{\omega}(0)^2} \quad (58) \end{aligned}$$

Remark 4 The following conclusions can be made based on (1):

- (i) For any $c_3 > 0$, $c_4 > 0$, $\lambda > 0$, and $\Lambda > 0$, the boundedness of signals is guaranteed to be global and uniform. For the control design, the priori information of the parameter uncertainty is not required.
- (ii) To improve the displacement tracking performance, we may increase c_3 . However, this will increase the velocity tracking error. The small velocity tracking error can be achieved after fixing c_3 to some acceptable value and increasing c_4 or λ , and Λ simultaneously.

3.3 ζ_2 -Subsystem

Under the control laws (26) and (46), the ζ_2 -subsystem (11) can be described as

$$\dot{\varphi} = f(\gamma, \varphi, u) \quad (59)$$

where $\varphi = [\zeta_2, \dot{\zeta}_2]^T$, $\gamma = [\zeta_1, \zeta_3, \dot{\zeta}_1, \dot{\zeta}_3]^T$, and $u = [\tau_1, \tau_2]^T$.

Assumption 2 [38,42] The following function is Lipschitz in γ , i.e., there are some Lipschitz positive constants L_γ and L_f satisfying

$$\|C_{31}\dot{\zeta}_1 + g_3 + f_3(\dot{\zeta}_3) + d_3\| \leq L_\gamma \|\gamma\| + L_f. \quad (60)$$

In addition, γ converges to a small neighborhood of $\gamma_d = [\zeta_{1d}, \zeta_{3d}, \dot{\zeta}_{1d}, \dot{\zeta}_{3d}]^T$ in accordance with the stability analysis of ζ_1 and ζ_3 subsystems,

Lemma 1 [38,42] *If ζ_1 -subsystem and ζ_3 -subsystem are stable, then the ζ_2 -subsystem (11) is globally asymptotically stable as well.*

Now, it is straightforward to conclude the following theorem.

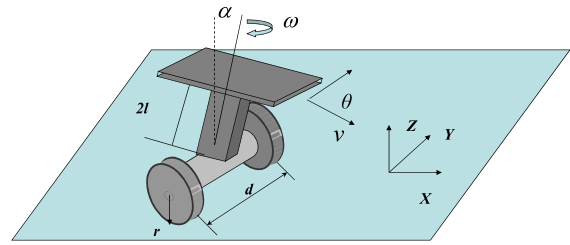


Fig. 1 WIP model [10]

Theorem 3 *Considering the system (10–12) with the control laws (26) and (46), for $(\zeta_1(0), \dot{\zeta}_1(0)) \in \Omega_{10}$ and $(\zeta_3(0), \dot{\zeta}_3(0)) \in \Omega_{30}$, where Ω_{10} and Ω_{30} are two compact sets, the tracking errors converge to a set which contains the origin with a rate at least $e^{-\nu t}$, and all the closed-loop signals are kept to be bounded.*

4 Simulation results

In the simulation, we consider a WIP system as shown in Fig. 1. The definitions of the parameters are as follows. R is the wheels radius, L is half length of the pendulum, D is the distance between two wheels, M is the pendulum and mobile platform mass, m is the each wheel mass, B is the ground friction coefficient, J_a and J are the inertia moment of the mobile platform and pendulum, and each wheel, respectively, g is gravity acceleration, θ is the angle of the mobile platform, α is the tilt angle of the pendulum, τ_l and τ_r are the torques on the left and right wheels, respectively.

The constraints on the WIP system are as follows. $\dot{x} \sin \theta - \dot{y} \cos \theta = 0$. We can obtain the reduced dynamics of α , $q_v = [\theta, x, y]^T$, $J_v = [0, \sin \theta, -\cos \theta]$, and $\dot{\zeta} = [\omega, \nu, \dot{\alpha}]^T$ through the Lagrangian approach. The corresponding matrices

$$\begin{aligned} \text{are } D_1 &= \begin{bmatrix} d_{11}(\zeta_3) & 0 & 0 \\ 0 & d_{22} & ML \cos \alpha \\ 0 & ML \cos \alpha & ML^2 + J_a \end{bmatrix}, C_1 = \\ &\begin{bmatrix} ML^2 \sin^2 2\alpha \dot{\alpha} / 2 & 0 & \omega ML^2 \sin 2\alpha / 2 \\ 0 & 0 & -ML \sin \alpha \dot{\alpha} \\ -\omega ML^2 \sin 2\alpha / 2 & 0 & 0 \end{bmatrix}, G_1 = [0, 0, \\ &-MgL \sin \alpha]^T, F_1 = \rho[\omega, \nu, 0]^T, \text{ where } d_{11}(\zeta_3) = \\ &D^2 m / 2 + JD^2 / 2R^2 + J_w + M^2 L^2 \sin^2 \alpha, d_{22} = \\ &2m + 2J / R^2 + M. \text{ In the simulation, the parameters} \\ &\text{are chosen as shown in Table 2. The initial states of} \\ &\text{the WIP are chosen as } \zeta(0) = [-0.1, 0, 10^\circ]^T, \text{ and} \\ &\dot{\zeta}(0) = [0.0, 0.05, 0.0]^T. \text{ The initial velocity of the} \end{aligned}$$

Table 2 Parameters in the simulation

M (kg)	J (kgm ²)	J_w (kgm ²)	J_a (kgm ²)	m (kg)	L (m)	D (m)	R (m)	ρ
12.0	1.2	4.5	1.8	1.80	1.0	1.0	0.5	diag[0.1]

Fig. 2 State response of the WIP. **a** Tilt angle of the WIP. **b** Tilt angle velocity of the WIP. **c** Forward velocity of the WIP. **d** Motion displacement of the WIP

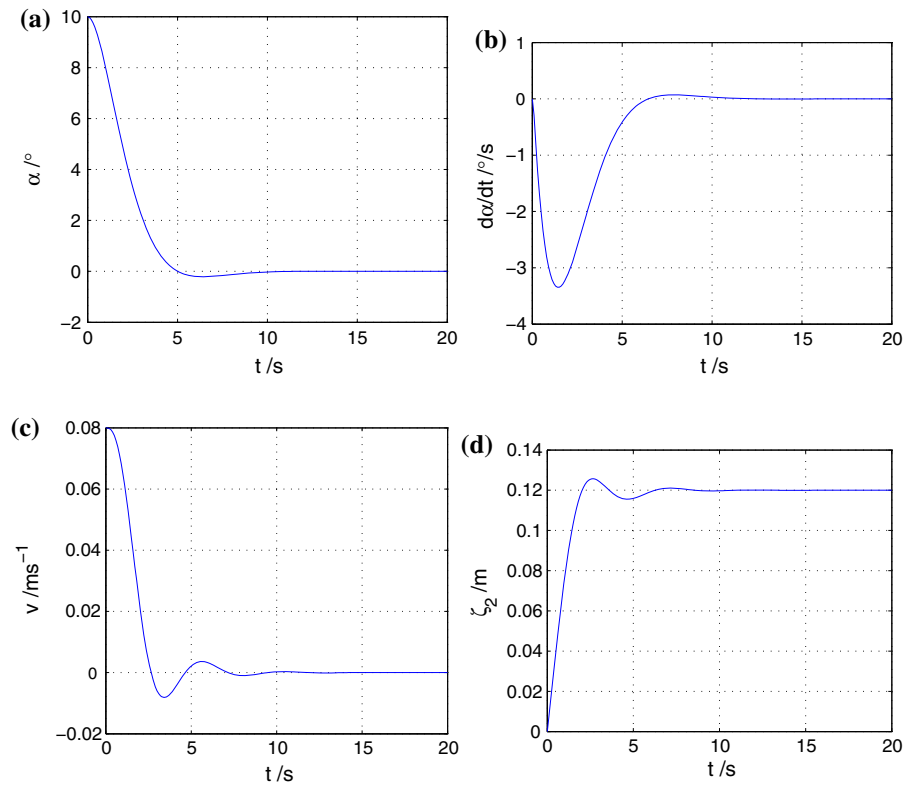
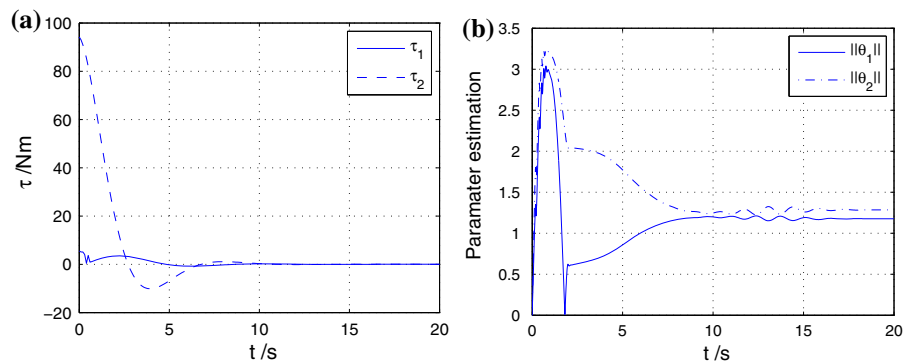


Fig. 3 Control inputs and the parameter estimation. **a** Control inputs of the WIP. **b** Parameter estimation of the WIP



WIP is 0.08m/s , and the desired trajectories are defined as $\theta_d = 0.4t$ rad and $\alpha_d = 0$ rad.

Simulation results are shown in Figs. 2 and 3. From the figures, we can find that the WIP can follow the desired trajectory under the proposed control law. The estimated parameter is convergence as time goes infinity. In addition, all the closed-loop signals are bounded.

5 Conclusion

We have presented adaptive backstepping control of the WIP system, while considering the model parameter uncertainties and the underactuated properties. The coordinates transformation has been employed to divide the system into three sub-systems. The back-

stepping control has been designed for each sub-system while the Lyapunov analysis has been involved in the control design and the stability proof. It has been proved that under the designed control law, the output trajectory is able to track as close as to the reference trajectory. All the signals have been ensured to be semi-globally uniformly ultimately bounded. Simulation results have shown the performance of the WIP control system as well.

Acknowledgments The authors would like to thank Professor Zhijun Li and Professor Chenguang Yang for their guidance and constructive comments for preparation of this paper, thank the editor and anonymous reviewers for their constructive suggestions and comments. This work was supported by the National Natural Science Foundation of China (NSFC) under Grant 51209174, 61472325 and 51311130137, the Fundamental Research Program of Northwestern Polytechnical University (NPU) under Grant JCY20130113, and the State Key Laboratory of Robotics and System (HIT) under Grant SKLRS-2012-MS-04.

References

- Chiu, C.-H.: The design and implementation of a wheeled inverted pendulum using an adaptive output recurrent cerebellar model articulation controller. *IEEE Trans. Industr. Electron.* **57**(5), 1814–1822 (2010)
- Li, Z., Kang, Y.: Dynamic coupling switching control incorporating support vector machines for wheeled mobile manipulators with hybrid joints. *Automatica* **46**(5), 832–842 (2010)
- Kim, Y., Kim, S.H., Kwak, Y.K.: Dynamic analysis of a nonholonomic two-wheeled inverted pendulum robot. *J. Intell. Robot. Syst.* **44**(1), 25–46 (2005)
- Grasser, F., D'Arrigo, A., Colombi, S., Rufer, A.C.: Joe: a mobile, inverted pendulum. *IEEE Trans. Ind. Electron.* **49**(1), 107–114 (2002)
- Pathak, K., Franch, J., Agrawal, S.K.: Velocity and position control of a wheeled inverted pendulum by partial feedback linearization. *IEEE Trans. Robot.* **21**(3), 505–513 (2005)
- Huang, J., Wang, H., Matsuno, T., Fukuda, T., Sekiyama, K.: Robust velocity sliding mode control of mobile wheeled inverted pendulum systems. In: *Proceedings of 2009 IEEE International Conference on Robotics and Automation, ICRA'09*, pp. 2983–2988. IEEE (2009)
- Li, Z., Yang, C.: Neural-adaptive output feedback control of a class of transportation vehicles based on wheeled inverted pendulum models. *IEEE Trans. Control Syst. Technol.* **20**(6), 1583–1591 (2012)
- Fierro, R., Lewis, F.L.: Control of a nonholonomic mobile robot using neural networks. *IEEE Trans. Neural Netw.* **9**(4), 589–600 (1998)
- Huang, J., Guan, Z.-H., Matsuno, T., Fukuda, T., Sekiyama, K.: Sliding-mode velocity control of mobile-wheeled inverted-pendulum systems. *IEEE Trans. Robot.* **26**(4), 750–758 (2010)
- Li, Z., Yang, C., Fan, L.: *Advanced Control of Wheeled Inverted Pendulum Systems*. Springer Publishing Company, Incorporated, Berlin (2013)
- Huang, C.-H., Wang, W.-J., Chiu, C.-H.: Design and implementation of fuzzy control on a two-wheel inverted pendulum. *IEEE Trans. Ind. Electron.* **58**(7), 2988–3001 (2011)
- Liu, Y.-J., Chen, C.L.P., Wen, G.-X., Tong, S.-C.: Adaptive neural output feedback tracking control for a class of uncertain discrete-time nonlinear systems. *IEEE Trans. Neural Netw.* **22**(7), 1162–1167 (2011)
- Takei, T., Imamura, R., Yuta, S.: Baggage transportation and navigation by a wheeled inverted pendulum mobile robot. *IEEE Trans. Ind. Electron.* **56**(10), 3985–3994 (2009)
- Yang, C.: Trajectory planning and optimized adaptive control for a class of wheeled inverted pendulum vehicle models. *IEEE Trans. Cybern.* **43**(1), 24–36 (2013)
- Li, Z., Xia, Y., Sun, F.: Adaptive fuzzy control for multilateral cooperative teleoperation of multiple robotic manipulators under random network-induced delays. *IEEE Trans. Fuzzy Syst.* **22**(2), 437–450 (2014)
- Li, Z.: Adaptive fuzzy output feedback motion/force control for wheeled inverted pendulums. *IET Control Theory Appl.* **5**(10), 1176–1188 (2011)
- Reyhanoglu, M., van der Schaft, A., McClamroch, N.H., Kolmanovsky, I.: Dynamics and control of a class of underactuated mechanical systems. *IEEE Trans. Autom. Control* **44**(9), 1663–1671 (1999)
- Sampei, M., Tamura, T., Kobayashi, T., Shibui, N.: Arbitrary path tracking control of articulated vehicles using nonlinear control theory. *IEEE Trans. Control Syst. Technol.* **3**(1), 125–131 (1995)
- Acosta, J.A., Ortega, R., Astolfi, A., Mahindrakar, A.D.: Interconnection and damping assignment passivity-based control of mechanical systems with underactuation degree one. *IEEE Trans. Autom. Control* **50**(12), 1936–1955 (2005)
- Grizzle, J.W., Moog, C.H., Chevallereau, C.: Nonlinear control of mechanical systems with an unactuated cyclic variable. *IEEE Trans. Autom. Control* **50**(5), 559–576 (2005)
- Lin, W., Pongvuthithum, R., Qian, C.: Control of high-order nonholonomic systems in power chained form using discontinuous feedback. *IEEE Trans. Autom. Control* **47**(1), 108–115 (2002)
- Nakamura, Y., Mukherjee, R.: Nonholonomic path planning of space robots via a bidirectional approach. *IEEE Trans. Robot. Autom.* **7**(4), 500–514 (1991)
- Papadopoulos, E.: Path planning for space manipulators exhibiting nonholonomic behavior. In: *Proceedings of the International Conference on Intelligent Robots and Systems*, pp. 7–10 (1992)
- Guenard, N., Hamel, T., Mahony, R.: A practical visual servo control for an unmanned aerial vehicle. *IEEE Trans. Robot.* **24**(2), 331–340 (2008)
- Liljeback, P., Haugstuen, I.U., Pettersen, K.Y.: Path following control of planar snake robots using a cascaded approach. *IEEE Trans. Control Syst. Technol.* **20**(1), 111–126 (2012)
- Chen, M., Ge, S.S.: Direct adaptive neural control for a class of uncertain non-affine nonlinear systems based on disturbance observer. *IEEE Trans. Cybern.* **43**(4), 1213–1225 (2013)
- Yang, C., Ganesh, G., Haddadin, S., Parusel, S., Albuschaeffer, A., Burdet, E.: Human-like adaptation of force

- and impedance in stable and unstable interactions. *IEEE Trans. Robot.* **27**(5), 918–930 (2011)
28. Crespi, A., Lachat, D., Pasquier, A., Ijspeert, A.J.: Controlling swimming and crawling in a fish robot using a central pattern generator. *Auton. Robots* **25**(1–2), 3–13 (2008)
 29. Zhang, M., Tarn, T.-J.: Hybrid control of the pendubot. *IEEE/ASME Trans. Mechatron.* **7**(1), 79–86 (2002)
 30. Salerno, A., Angeles, J.: The control of semi-autonomous two-wheeled robots undergoing large payload-variations. In: Proceedings of the IEEE International Conference on Robotics and Automation, 2004. ICRA'04. 2004, vol. 2, pp. 1740–1745. IEEE (2004)
 31. Blankespoor, A., Roemer, R.: Experimental verification of the dynamic model for a quarter size self-balancing wheelchair. In: Proceedings of the 2004 American Control Conference, 2004, vol. 1, pp. 488–492. IEEE (2004)
 32. Liu, Y.-J., Tong, S.-C., Chen, C.L.P.: Adaptive fuzzy control via observer design for uncertain nonlinear systems with unmodeled dynamics. *IEEE Trans. Fuzzy Syst.* **21**(2), 275–288 (2013)
 33. Chen, M., Ge, S.S., Voon Ee How, B.: Robust adaptive neural network control for a class of uncertain mimo nonlinear systems with input nonlinearities. *IEEE Trans. Neural Netw.* **21**(5), 796–812 (2010)
 34. Liu, Y.-J., Li, Y.-X.: Adaptive fuzzy output-feedback control of uncertain siso nonlinear systems. *Nonlinear Dyn.* **61**(4), 749–761 (2010)
 35. Li, Z., Yang, C., Su, C.-Y., Ye, W.: Adaptive fuzzy-based motion generation and control of mobile under-actuated manipulators. *Eng. Appl. Artif. Intell.* **30**, 86–95 (2014)
 36. Yang, C., Ma, H., Fu, M.: Adaptive predictive control of periodic non-linear auto-regressive moving average systems using nearest-neighbour compensation. *IET Control Theory Appl.* **7**(7), 936–951 (2013)
 37. Chen, M., Wu, Q., Jiang, C.: Disturbance-observer-based robust synchronization control of uncertain chaotic systems. *Nonlinear Dyn.* **70**(4), 2421–2432 (2012)
 38. Li, Z., Zhang, Y.: Robust adaptive motion/force control for wheeled inverted pendulums. *Automatica* **46**(8), 1346–1353 (2010)
 39. Yang, C., Li, Z., Cui, R., Xu, B.: Neural network-based motion control of an underactuated wheeled inverted pendulum model. *IEEE Trans. Neural Netw. Learn. Syst.* (2014). doi:[10.1109/TNNLS.2014.2302475](https://doi.org/10.1109/TNNLS.2014.2302475)
 40. Chiu, C.-H., Lin, Y.-W., Lin, C.-H.: Real-time control of a wheeled inverted pendulum based on an intelligent model free controller. *Mechatronics* **21**(3), 523–533 (2011)
 41. Chiu, C.-H.: Self-tuning output recurrent cerebellar model articulation controller for a wheeled inverted pendulum control. *Neural Comput. Appl.* **19**(8), 1153–1164 (2010)
 42. Li, Z., Zhang, Y., Yang, Y.: Support vector machine optimal control for mobile wheeled inverted pendulums with unmodelled dynamics. *Neurocomputing* **73**(13), 2773–2782 (2010)
 43. Krstic, M., Kanellakopoulos, I., Kokotovic, P.V., et al.: *Nonlinear and Adaptive Control Design*. Wiley, New York (1995)